

## **Nuclear Design Methodology of Fission Moly Target for Research Reactor**

**Dong-Keun Cho and Myung-Hyun Kim**

Kyunghee University  
Kiheung-eup, Yongin 449-701, Korea  
mhkim@nms.kyunghee.ac.kr

**Dong-Seong Sohn**

Korea Atomic Energy Research Institute  
150 Dukjin-dong, Yusong-gu, Taejon 305-353, Korea

(Received December 14, 1998)

### **Abstract**

A nuclear design of fission moly production targets for a research reactor, HANARO was performed. It was found that the use of MCNP-4A, ORIGEN-2 code was reliable for the analysis of production characteristics of  $^{99}\text{Mo}$  in a target fuel at an irradiation holes. A parametric study was done for the optimization of target location, target dimension, target shape and fuel materials. It was shown that a fuel thickness was the most sensitive parameters and electro-deposited target gave the highest  $^{99}\text{Mo}$  yield ratio. A pellet target with vibro-compaction powder, however, showed the largest production capacity and better engineering feasibility even with less yield ratio. Ten kinds of optimized target design for both LEU and HEU satisfied all the given design constraints. The most favorable design was the HEU ring-shaped electro-deposited target, considered the safety limit, production yield, chemical process easiness, yield ratio, and amount of radioactive waste.

**Key Words** : isotope production, molybdenum-99, technetium-99, nuclear design, fission moly, target

### **1. Introduction**

Molybdenum-99 is a parent isotope of technetium-99m which has been widely used in clinical nuclear imaging procedures.  $^{99m}\text{Tc}$  emits monoenergetic 140-keV photons with relatively short half-life of 6 hours, which makes diagnostic dose level the minimum and processed images the best[1,2]. Because  $^{99}\text{Mo}$  has a 67-hour half-life, it

cannot be stockpiled. This is the why a steady supply of  $^{99}\text{Mo}/^{99m}\text{Tc}$  generators is crucial to the industry of nuclear medicine. Commercial production of  $^{99}\text{Mo}$ , however, has been almost exclusively dependent upon NRU reactor operated by AECL and Nordion. Therefore, a need for a reliable regional supply facility was recognized. The U.S. Department of Energy decided to convert a research reactor, Annular Core

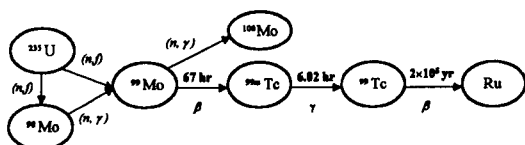


Fig. 1. Production-Destruction Scheme of  $^{99}\text{Mo}$  in a Fission Moly Target

Research Reactor at Sandia National Laboratories into a dedicated  $^{99}\text{Mo}$  supplier[3].

Molybdenum-99 can be produced in two ways. The conventional method of neutron capture is a simple and inexpensive way. However, the specific activity(Ci  $^{99}\text{Mo}$ /gMo) of products is very low because of the small cross section of  $(n, \gamma)$  reaction. Therefore, this method has not been used for massive commercial production. On the contrary, nuclear fission method is a more favorable method which guarantees a high specific activity and a mass production capacity, although it produces large amounts of radioactive waste and requires remarkable initial capital investment[4].

Recently, Korea Atomic Energy Research Institute (KAERI) performed a feasibility study for a fission moly production in High-flux Advanced Neutron Application Reactor (HANARO)[5]. In this study, KAERI concluded that commercial molybdenum production would be competitive as a regional backup supplier, if the capacity should exceed 60,000 Ci per year[6].

In this paper, a parametric study for the target design optimization of dimensions, shapes, locations and material was done. A feasibility of optimized candidate targets was also investigated under the irradiation facility condition of HANARO.

## 2. Behavior of $^{99}\text{Mo}$ in a Fission Moly Target

$^{99}\text{Mo}$  is formed as a result of nuclear fission of  $^{235}\text{U}$  and neutron capture of  $^{98}\text{Mo}$  produced from

nuclear fission in a target, as shown in Fig. 1.

Considered the decay of  $^{99}\text{Mo}$  and  $^{99}\text{Mo}(n, \gamma)^{100}\text{Mo}$  reaction, we set up a  $^{99}\text{Mo}$  material balance in terms of number densities  $N_i$ :

$$\frac{dN^{99}}{dt} = \gamma^{99} N^{235} \sigma_f^{235} \phi + \sigma_r^{98} N^{98} \phi - \lambda^{99} N^{99} - \sigma_r^{99} N^{99} \phi \quad (1)$$

$$\frac{dN^{98}}{dt} = \gamma^{98} N^{235} \sigma_f^{235} \phi - \sigma_r^{98} N^{98} \phi \quad (2)$$

where,  $\gamma^i$ : fission yield fraction of nuclide  $i$ ,

$\sigma_r^i$ : capture cross section of nuclide  $i$ ,

$N^i$ : number density of nuclide  $i$  at time  $t$ ,

$\sigma_f^i$ : microscopic fission cross section of nuclide  $i$ ,

$\lambda^i$ : decay constant of nuclide  $i$ ,

$\phi$ : neutron flux,

and the superscripts 98, 99 and 235 represent  $^{98}\text{Mo}$ ,  $^{99}\text{Mo}$  and  $^{235}\text{U}$ , respectively. Assuming that microscopic absorption cross section,  $\sigma_a^{235}$ , and neutron flux are constant to the time, the  $^{235}\text{U}$  number density at time  $t$  is given by the relationship:

$$N^{235}(t) = N_0^{235} e^{-\sigma_a^{235} \phi \cdot t} \quad (3)$$

where  $N_0^{235}$  is the number density of  $^{235}\text{U}$  at  $t=0$ .

Integrating Eqs. (1) and (2) to the time from zero to  $t$  after inserting Eq. (3) into Eq. (1), (2), and applying the zero-existence conditions of  $^{99}\text{Mo}$  and  $^{98}\text{Mo}$  at  $t=0$ , we can derive the equation for  $N^{99}(t)$ .

$$\begin{aligned} N^{99}(t) = & \gamma^{99} \left[ \frac{N_0^{235} \sigma_f^{235} \phi}{\lambda^{99} + \sigma_r^{99} \phi - \sigma_a^{235} \phi} \right] \\ & \times (e^{-\sigma_a^{235} \phi \cdot t} - e^{-(\lambda^{99} + \sigma_r^{99} \phi) \cdot t}) \\ & + \gamma^{98} \left[ \frac{N_0^{235} \sigma_f^{235} \phi}{\lambda^{99} + \sigma_r^{98} \phi - \sigma_a^{235} \phi} \right] \\ & \times \left[ \frac{\sigma_r^{98}}{\sigma_r^{98} - \sigma_a^{235}} \right] \\ & \times (e^{-\sigma_a^{235} \phi \cdot t} - e^{-(\lambda^{98} + \sigma_r^{98} \phi) \cdot t}) \end{aligned} \quad (4)$$

$$\begin{aligned}
& + \gamma^{98} \left[ \frac{N_0^{235} \sigma_f^{235} \phi}{\lambda^{99} + \sigma_r^{99} \phi - \sigma_r^{98} \phi} \right] \\
& \times \left[ \frac{\sigma_r^{98}}{\sigma_r^{98} - \sigma_a^{235}} \right] \\
& \times (e^{-\sigma_r^{98} \phi \cdot t} - e^{-(\lambda^{99} + \sigma_r^{99} \phi) \cdot t})
\end{aligned}$$

Values of  $\sigma_r^{98}$  and  $\sigma_r^{99}$  at 0.0253 eV are 0.13b and 8b, those are much less than  $\sigma_a^{235}$ . Therefore, the second and third term of the above equation is

about  $\frac{1}{5000}$  of the first term. The approximate

form of Eq. (4) can be written in terms of activity(Ci  $^{99}\text{Mo}/\text{cm}^3$ ).

$$\begin{aligned}
\lambda^{99} N_{99}(t) & \cong \lambda^{99} \frac{\gamma^{99} N_0^{235} \sigma_f^{235} \phi}{\lambda^{99} + \sigma_r^{99} \phi - \sigma_a^{235} \phi} \\
& \times (e^{-\sigma_a^{235} \phi \cdot t} - e^{-(\lambda^{99} + \sigma_r^{99} \phi) \cdot t})
\end{aligned} \quad (5)$$

From Eq. (5), it is found that  $^{99}\text{Mo}$  activity reaches its certain maximum value after  $t$  second irradiation. The time to the saturation can be found as the following.

$$t = \frac{\ln \left( \frac{\lambda^{99} + \sigma_r^{99} \phi}{\sigma_a^{235} \phi} \right)}{\lambda^{99} + \sigma_r^{99} \phi - \sigma_a^{235} \phi} \quad (6)$$

Assuming that neutron flux is  $1 \times 10^{13} \text{ \#}/\text{cm}^2\text{-sec}$  and neutron absorption cross section of  $^{235}\text{U}$  is 683.2 barns at 0.0253 eV, the saturation time is about 24 days. However, it is found that the  $^{99}\text{Mo}$  activity comes up to 71% and 83% of its maximum value only after 5 and 7 days irradiation, respectively.

In Eq. (6), the higher the flux level is, the more the saturation time is shortened. Assuming that neutron flux is  $1 \times 10^{14} \text{ \#}/\text{cm}^2\text{-sec}$ , the saturation time becomes about 15 days. In this case,  $^{99}\text{Mo}$  activity comes up to 77% and 88% of its maximum value after 5 and 7 days irradiation. It is

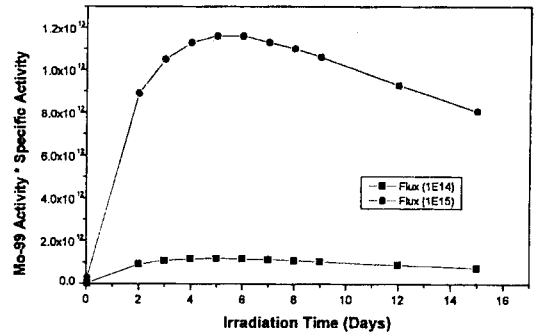


Fig. 2. A Change of  $^{99}\text{Mo}$  Activity Times Specific Activity to the Irradiation Time

also found that enrichment and neutron flux must be as high as possible to obtain high yield ratio(Ci  $^{99}\text{Mo}/\text{gU}$ ) from the Eq. (5). A higher  $^{235}\text{U}$  enrichment makes the yield ratio high, which means high enriched uranium(HEU) is more favorable also in the radioactive waste production.

It is known that longer irradiation time results in lower specific activity because of the formation of stable molybdenum isotopes from fission.  $^{99}\text{Mo}$  activity times specific activity to the irradiation time is shown in Fig. 2. It is found that irradiation span of 4~7 days indicates the most favorable target quality condition.

### 3. Design Tool

From Eq. (5), the factors affecting the  $^{99}\text{Mo}$  production are initial  $N^{235}$  number density, neutron flux and irradiation time. For the evaluation of target design, correct estimation of flux throughout the target geometry is crucial. In this paper, fission reaction rates in a target were evaluated by MCNP-4a. A 3-dimensional whole reactor core including irradiation thimble, beam tube, and reflector tank was described in detail heterogeneously. Whenever target modeling was changed, KCODE simulation was performed to reflect the varied source in the target. A detailed calculations to obtain the fission reaction rate were

done with variance reduction techniques. A  $^{99}\text{Mo}$  activity in an irradiated target was evaluated by ORIGEN-2 assuming that fission reaction rate is invariant during the 7-days irradiation period. It was assumed that average neutron flux level at the target hole be constant during a period of irradiation and that fission yield fraction of  $^{99}\text{Mo}$  be invariant for the different incident neutron energy. However, it is expected that the difference due to these assumption will be small enough compared to the design parameter changes, since  $N^{235}$  number density varies a little resulting from the short irradiation period.

#### 4. Parametric Study

The most effective production method of  $^{99}\text{Mo}$  is known to be the extraction method from fission products of HEU target fuel. The U.S. company Cintichem had produced molybdenum from HEU before 1991. Current vendors, Nordion in CANADA and IRE in Belgium also use HEU target. Reduced Enrichment for Research and Test Reactors (RERTR) program, however, has encouraged all member countries to use low enriched uranium (LEU) for fission moly target fuel as well as for fuels of research and test reactors. Except for RERTR program recommendation, the use of HEU is restricted in Korea. An international agreement on safeguards should be guaranteed with on the stable supply of HEU. Therefore, target design should be done for LEU as well as HEU.

In the following parametric study, target design parameters were tested when targets were loaded at the outer core irradiation holes.

##### 4.1. LEU Target Design Parameters

For the optimization of target design, yield ratio( $\text{Ci } ^{99}\text{Mo/gU}$ ) and surface heat flux(SHF) were

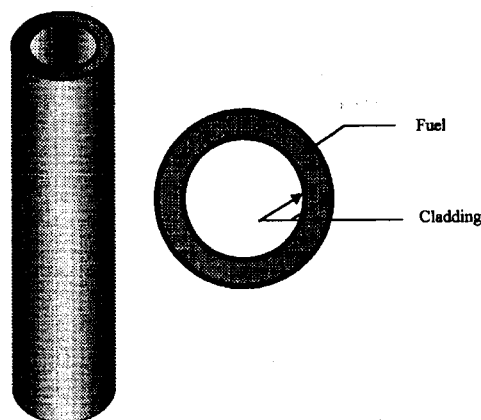
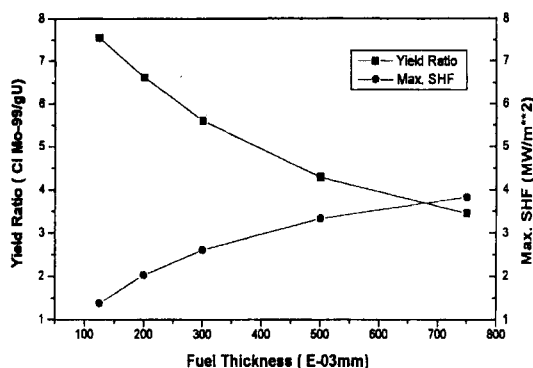


Fig. 3. Conceptual Fission Moly Target Model

compared for the change of the target irradiation location, axial length, target fuel thickness, target geometry, and fuel materials. A reference target used in this parametric study is a hollow sintered pellet type with 19.75w/o UN which is designed to be cooled by both inner and outer surface.

##### 4.1.1. Axial Length and Irradiation Location

Excess reactivity in HANARO is controlled by regulating rods for the 28 days reload cycle, therefore rods insertion positions are varying a little even for an irradiation period of 7 days concurrent with a little change of axial flux shape.  $^{99}\text{Mo}$  yield ratio can be different for the change of target length and axial location in the hole during four-reloading time, 28 days. A sensitivity of  $^{99}\text{Mo}$  yield ratio was investigated to these two factors. It was assumed that target have the thickness of  $500\mu\text{m}$  with theoretical density. The axial length of 30, 40 and 50cm was considered in a 70cm core height and positions of target are set to have flux as high as possible. It was known that axial length of 30cm and 50cm made  $^{99}\text{Mo}$  yield ratio 4% higher and 5% lower respectively compared with 40cm. Bottom-shifted irradiation location was a little



**Fig. 4. Variation of  $^{99}\text{Mo}$  Yield Ratio and Maximum SHF to the Change of Target Fuel Thickness**

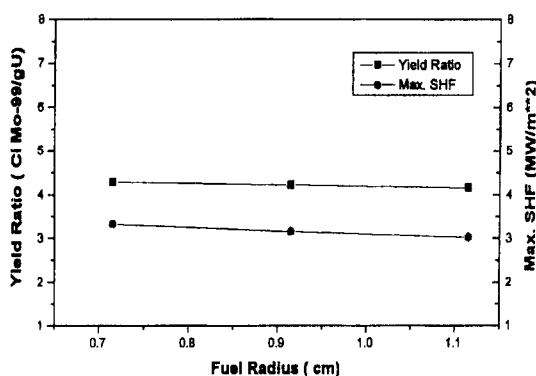


**Fig. 5. Variation of  $^{99}\text{Mo}$  Yield Ratio and Maximum SHF to the Change of Fuel Size**

advantageous, but the gain of yield ratio is only about 1%. The results of surface heat flux (SHF) to these parameters showed almost the same results as of yield ratio. It was found that axial length and target elevation were not the key factors to the yield ratio and SHF.

#### 4.1.2. Target Geometry

A parametric study for geometry was done to the variation of thickness and size of the fuel. Conceptual model is shown in Fig. 3.

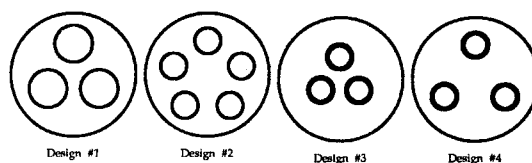


**Fig. 6. Four Geometrical Models of Target Designs**

Fig. 4 and Fig. 5 show the variation of yield ratio and maximum SHF to the thickness and size change, respectively. In the Fig. 4, it was assumed that target have 1.15cm of inner diameter with theoretical density, and in the Fig. 5, 500  $\mu\text{m}$  of thickness. Axial length was 40cm, and target is positioned at 7.5cm height from the bottom of the hole, i.e. at the slightly bottom-shifted location, reflecting the previous results.

As shown in Fig. 4, the higher yield ratio was expected as the thickness became thinner, especially, in the range of several hundreds micrometers, but it was relatively insignificant in the range of several thousands micrometers in LEU target. This results is due to spatial self-shielding effect. As expected, thinner thickness of the fuel also showed lower SHF.

As shown in Fig. 5, both the yield ratio and the SHF were almost insensitive to the radius change.

Design #1 through 4 in Fig. 6 has the same amount of uranium fuel. Target of design #2 has the smaller radius than that of design #1, which makes the design #2 have more number of targets than those of #1, where both design have the same fuel thickness. The differences between design #2 and 3 are the fuel thickness and the number of targets. Because design #3 is thicker than that of design #2, design #3 has the less number of targets. design #3 and 4 was modeled

**Table 1. Yield Ratio and Surface Heat Flux**

Design #	1	2	3	4
Yield Ratio (Ci <sup>99</sup> Mo/gU)	5.939	5.977	5.460	5.471
Max. SHF (MW/m <sup>2</sup> )	1.311	1.323	1.996	1.999

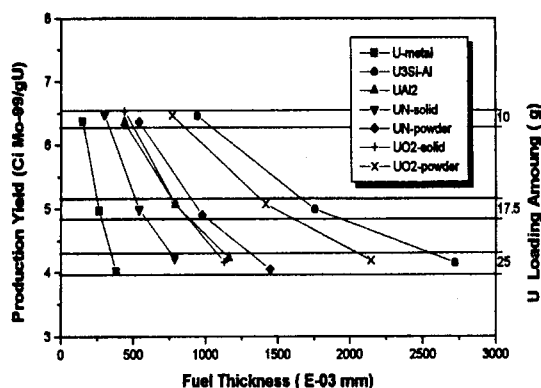
to evaluate the effect caused by radial arrangement of target.

Table 1 compares yield ratio and SHF of these 4 designs. As expected, design #1 and 2 gave the same yield ratio, and design #3 gave the lower yield ratio than that of design #2 which has thinner fuels. In the case of SHF, design #1 was more favorable than design #2, and design #3 which gave higher SHF. It is found that larger radius, thinner thickness of the fuel, smaller number of target are preferable for a given amount of fuel.

#### 4.1.3. Fuel Material

As a target materials, many kinds of fuel materials were considered; UO<sub>2</sub> powder compacted in double tubes, UO<sub>2</sub> hollow pellet type, U metal plate type developed at ANL, U<sub>3</sub>Si-Al type, U/Al alloy target used in Nordion, and UN powder or pellet type, etc. For each material mentioned above, <sup>99</sup>Mo yield ratios, surface heat fluxes, production rates, and quantities of radioactive waste were evaluated.

Geometry modeled to evaluate a characteristics of each fuel material was treated as follows; Outer radius of the fuel was fixed and inner radius of the fuel was adjusted to cause the target to be loaded with the equivalent amount of uranium to each material. Target axial length is same throughout the all case. In a Fig. 7, <sup>99</sup>Mo yield ratio was shown for each materials, which



**Fig. 7. Variation of <sup>99</sup>Mo Yield Ratio to the Change of Thickness of Each Fuel Materials**

showed the almost same yield ratio regardless of each fuel material once enrichment and the amount of uranium was the same. Therefore, in the Table 2, it was shown that UO<sub>2</sub> powder in double tube type should be fabricated at the thickness of 770  $\mu$ m to derive equivalent yield ratio induced by metal fuel at 150  $\mu$ m. Similarly, only if UO<sub>2</sub> powder is fabricated at the thickness of 2,145  $\mu$ m, the same yield ratio will be expected in metal fuel at 381  $\mu$ m. However, powder can not be packed in the narrow space of the double tube. If small quantities of <sup>99</sup>Mo is required to be produced at the limited irradiation sites, uranium amount per target can be reduced. In this case, metal fuel or U/Al alloy is more desirable, because it could be fabricated thin. U/Al alloy, however, has disadvantage of large quantities of waste caused by a large Al content and much recoil loss of <sup>99</sup>Mo to the Al matrix. Even if U metal gave high yield ratio, it is difficult for U metal to be separated from cladding tubes as a thin foil[7].

In the Fig. 7, the thinner thickness results in the less fuel loading amount, which causes less amount of the <sup>99</sup>Mo production, but results in the higher yield ratio. Thus, the highest yield ratio

**Table 2.  $^{99}\text{Mo}$  Yield Ratio and Thickness of Each Material (numbers in the parenthesis are thickness in  $\mu\text{m}$ )**

Material $^{235}\text{U}$ Loading	U-metal	$\text{U}_3\text{Si-Al}$	$\text{U/Al}_2$ alloy	UN-solid (70 %T.D.)	UN-powder (40 %T.D.)	$\text{UO}_2$ -solid (70 %T.D.)	$\text{UO}_2$ -powder (40 %T.D.)
10 g	6.374 (150)	6.453 (943)	6.351 (440)	6.472 (304)	6.361 (541)	6.526 (430)	6.463 (770)
17.5 g	4.975 (264)	4.993 (1,758)	5.061 (791)	4.985 (541)	4.901 (978)	5.094 (771)	5.075 (1,417)
25 g	4.108 (381)	4.153 (2,720)	4.226 (1,162)	4.225 (787)	4.053 (1,449)	4.163 (1,131)	4.189 (2,145)

could be obtained by electro-deposited method which can make the thinnest fuel layer. It is, however, inappropriate for the massive moly production because of its engineering deposition thickness limit.

The powder compacted fuel was proven to be the more favorable fuel whose performance are competitive with the metal fuel, when it is used for a large scale production. It is expected to have the benefits of simple fabrication compared with metal fuel and rapid dissolution from the large surface area contacting with chemical agent.

#### 4.2. HEU Target Design Parameters

It is advantageous to use HEU for a fission moly target fuel material because of its higher yield ratio and lower quantities of radioactive waste than LEU. Furthermore, HEU is favorable because it produces plutonium about 54 times less than that of LEU. With the limited assumption of usage, target design study was done for HEU target.

For the effective HEU target design, design parameters was analyzed like that was done LEU. From this study, effectiveness of HEU was shown within limited thickness of fuel,  $100\mu\text{m}$  because of higher special self-shielding effect than that of LEU. HEU target, therefore, should be fabricated

by electro-deposited method to achieve high  $^{99}\text{Mo}$  yield.

### 5. Optimum Target Design in HANARO

Based on the previous parametric studies, a nuclear design was performed for the targets satisfying the operational constraints in HANARO.

#### 5.1. Design Constraints

HANARO is a 30 MWt open-tank-in-pool-type reactor loaded with 19.75w/o dispersed fuels( $\text{U}_3\text{Si}$  is dispersed in Al matrix). Reactor core and 8 outer-core irradiation tubes are cooled by forced convection of light water. 2 out of 8 irradiation holes are designated for target irradiation. The average thermal neutron flux( $<0.625\text{eV}$ ) in the hole is measured to be about  $3.36 \times 10^{14}\text{\#}/\text{cm}^2\text{-sec}$ . Inlet and outlet coolant temperature of tubes are  $35^\circ\text{C}$  and  $45^\circ\text{C}$ , respectively. The axial length of the irradiation tube made of zircaloy-4, is 112cm, and the inner diameter is 60mm. The large volume of  $\text{D}_2\text{O}$  reflector around the core prevents fast and epithermal neutrons from escaping and provides sufficient thermal neutrons for a irradiation site.

Target is to be loaded at the on-power condition, and a facility for loading/unloading of target fuels

**Table 3. Designed LEU Assembly Targets**

Design #	Rod #/Ass.	% T.D.	Fuel Mat.	Outer Clad.		Fuel Thickness( $\mu$ m)	Inner Clad.	
				O.R.(mm)	I.R.(mm)		O.R.(mm)	I.R.(mm)
L-1	3	100	U metal	11.33	10.9	125	10.77	10.42
L-2	3	100	UO <sub>2</sub> electro-deposited	11.33	10.9	140	10.75	10.41
L-3	3	100	"	11.33	10.9	150	10.74	10.40
L-4	3	100	"	11.33	10.9	160	10.73	10.39
L-5	3	30	UO <sub>2</sub> powder	11.33	10.9	1,400	9.50	9.15

**Table 4. <sup>99</sup>Mo Yield Ratio and SHF from Designed LEU Assemblies**

Design #	Total U-235 Loading (g)	Reactivity Worth (% $\Delta\rho$ )	Avg. LHR (Kw/m)	Max. SHF (MW/m <sup>2</sup> )	Yield Ratio (Ci <sup>99</sup> Mo/gU)	<sup>99</sup> Mo Yield (Ci/year)
L-1	77.87	0.4223 $\pm$ 0.0684	182.6	1.775	6.149	96,960
L-2	43.62	0.2352 $\pm$ 0.0692	124.6	1.208	7.487	66,130
L-3	46.70	0.2573 $\pm$ 0.0616	130.8	1.253	7.342	69,455
L-4	49.80	0.3820 $\pm$ 0.0676	134.9	1.317	7.103	71,598
L-5	123.2	0.4253 $\pm$ 0.0710	244.6	2.451	5.205	129,700

is now being developed. In order not to meet departure from nucleate boiling, target must be cooled after loading, as well as, when it is being loaded. Based on the preliminary study, it is known that the reactor safety can be guaranteed only when reactivity worth by one target fuel assembly addition is less than 1.25%  $\Delta\rho$ . Additionally, maximum surface heat flux (SHF) should not exceed 2.76 MW/m<sup>2</sup>.

HANARO should be reloaded at every 35 day cycle(28 days operation and 7 days outage). Because target should be irradiated at least 7 days for Mo production, about 40 times of target loading can be expected. A commercial production capacity of 60,000 Ci/yr should be assured for the operational economics by 6 day reference (1 day is assumed for cooling after irradiation, 1 day for chemical process, and the 6-day period is reversed for delivery). Irradiated target should be treated by chemical process which produces large amount of liquid waste. A high

yield ratio is the key design factor in order to produce less amounts of radioactive waste and higher quality of <sup>99</sup>Mo.

## 5.2. LEU Target Assembly Design

Effective target design was performed with three acceptable candidate on the basis of previous study; electro-deposited, metal, and powder target. All designed target was assumed to be double tube hollow type which is cooled by both inner and outer surface. Its axial length is 40cm. The dimension of designed target assembly and their performance are shown in Table 3 and 4, respectively. The number of irradiation hole is limited to be two. Metal target was manufactured with uranium metal foil embedded in different two tubes, conceptually designed in Design L-1. In Design L-2~L-4, electro-deposited target was fabricated by inserting the small tube to the large tube and by welding the both edges. Inner surface



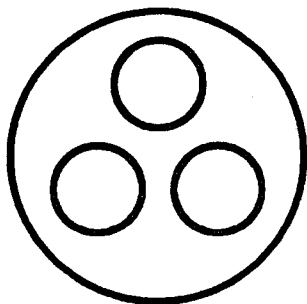


Fig. 8. Ring Type HEU Target

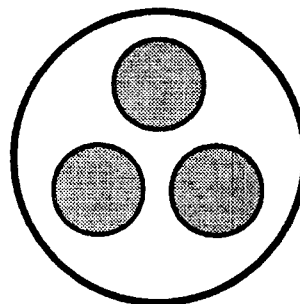


Fig. 9. Tube Type HEU Target

Table 5.  $^{99}\text{Mo}$  Yield Ratio and SHF from Designed HEU Assemblies

Design #	Type.	Fuel Film Thickness ( $\mu\text{m}$ )	Total U Loading (g)	Reactivity Worth ( $\% \Delta \rho$ )	Avg. LHR ( $\text{kW/m}$ )	Max. SHF ( $\text{MW/m}^2$ )	Yield Ratio ( $\text{Ci } ^{99}\text{Mo/gU}$ )	$^{99}\text{Mo}$ Yield ( $\text{Ci/year}$ )
H-1	Tube	50	58.7	$0.324 \pm 0.0638$	130.3	2.356	29.45	69,230
H-2	"	60	70.5	$0.407 \pm 0.0732$	146.1	2.672	27.52	77,600
H-3	Ring	50 (25+25)	58.7	$0.298 \pm 0.0573$	135.5	1.267	30.63	71,900
H-4	"	60 (30+30)	70.5	$0.302 \pm 0.0638$	153.2	1.552	28.87	81,400
H-5	"	120 (60+60)	238.9	$0.457 \pm 0.0601$	238.9	2.200	22.57	125,680

of the large tube and outer surface of the small tube were electro-plated by the film of  $\text{UO}_2$ .  $\text{UO}_2$  powder was vibro-compacted between two zircaloy tubes in Design L-5.

All designed target was maintained within the acceptable design constraints; less than  $1.25\% \Delta \rho$ , and  $2.76 \text{ MW/m}^2$  as shown in tables 3 and 4. We concluded that LEU  $\text{UO}_2$  electro-deposited target was the most favorable design if two irradiation hole would be used.  $\text{UO}_2$  powder target (Design L-1) resulted in high total production yield which satisfied production goal even with only one irradiation hole.

### 5.3. HEU Target Assembly Design

From the HEU parametric study, two types of

target were proposed. One was tube shape type just like Cintichem target and the other was ring shape type conceptually proposed. It was assumed that tube type target was fabricated just like Cintichem target, as shown Fig. 8. Ring type target had the same shape, as described for previous LEU deposited target, as shown Fig. 9. Designed target assembly was shown in Table 5.

Tube type target had electro-deposited fuel layer inside of 0.2 mm thickness stainless steel tube whose total outer diameter (O.D.) was 22.4 mm. In the ring type target, outer tube had the same dimension as tube type and inner tube had another layer of target fuel outside of 0.2 mm thickness stainless steel tube (Total O.D. was 22.0 mm). This target had two surfaces for cooling resulting in much less surface heat flux. It was

shown that both design satisfied the design constraints. Ring type target was a little favorable, because of its lower surface heat flux, higher total yield and larger surface area contacting chemical agent.

## 6. Conclusions

Design parameters was analyzed for the effective LEU target design. Target thickness was a key design parameter which controlled  $^{99}\text{Mo}$  yield ratio and SHF. The larger radius, thinner thickness of the fuel, smaller number of target was preferable for the higher yield ratio and lower SHF. Electro-deposited target could be designed with the highest yield ratio, but it was inappropriate for a massive production capacity. Powder compaction target was shown to be one of the practical options, for a large scale production from LEU targets.

Optimization of target design was done both LEU and HEU under the limited conditions. Compared LEU with HEU, HEU gave about 4 times higher  $^{99}\text{Mo}$  yield ratio than LEU. When only the engineering productivity was considered, HEU electro-deposition target was the most competitive choice of target.

## References

1. Dan Glenn, A. Sharif Heger and William B. Hladik III, "Comparison of Characteristics of Solution and Conventional Reactors for  $^{99}\text{Mo}$  Production," *Nucl. Tech.*, Vol. **118**, pp. 142-150, May (1997).
2. J. H. Park, et. al., "A Review on the Process Technology for Mo-99 Production," KAERI, KAERI-AR-401/94, (1994).
3. Richard L. Coats and Edward J. Parma, "Medical Isotope Production: A New Research Initiative for the Annular Core Research Reactor," *Proceedings of the 1994 Topical Meeting on Advances in Reactor Physics*, Knoxville, Tennessee, April 11-15 (1994).
4. S. C. Mo "Production of  $^{99}\text{Mo}$  Using LEU and Molybdenum Targets in a 1MW TRIGA Reactor," *Proc. 16th Int. Mtg. on Reduced Enrichment for Research and Test Reactors*, October 4-7, 1993, Oarai, Japan, JAERI-M 94-042, pp. 394-400, March (1994).
5. B. M. Yoon, et. al., "Development of Fission Mo Production Technology," KAERI, KAERI-RR-1752/96, (1996).
6. B. K. Kim, et. al., "Feasibility Study on Fission Moly Target Development," KAERI, KAERI/RR-1595/95, (1996).
7. G. L. Hofman, T. C. Wiencek, E. L. Wood, J. L. Snelgrove, "Development of  $^{99}\text{Mo}$  Isotope Production Targets Employing Uranium Metal Foils," *Trans. Am. Nucl. Sci.* 77, pp. 100-101, November, (1997).
1. Dan Glenn, A. Sharif Heger and William B.